3D Surface Measurement by Low Voltage Scanning Electron Microscope

T. Vynnyk; J. Seewig; E. Reithmeier
University Hannover, Institute of Measurement and Automatic Control.
Nienburgerstr. 17, 30167 Hannover, Germany
taras.vinnik@imr.uni-hannover.de

Abstract: An improved photometric method for recording a 3D-microtopography of technical surfaces is presented. The suggested procedure employs a scanning electron microscope (SEM) as multi-detector system. The improvement in measurement is based on the extended model of electron detection in 3D – space.

1. INTRODUCTION

Currently the optical measuring systems are admitted to be a standard measurement tool for area characterization. However, these devices have several weak points. The lateral resolution of every optical measurement device is limited by the wavelength of the light and lies in the range between 0.3 – 0.8 µm. Another restriction of the optical microscopes is the limited ability to measure the tilted areas. The optical measurements are based on the analysis of the light, reflected by the surface of the measured object. On the increase of tilt angle of the even but rough surface the part of the reflected light cone captured by the objective becomes sequentially smaller. When the critical angle is reached the signal to noise ratio becomes so bad that the surface cannot be stably detected anymore (Figure 1).

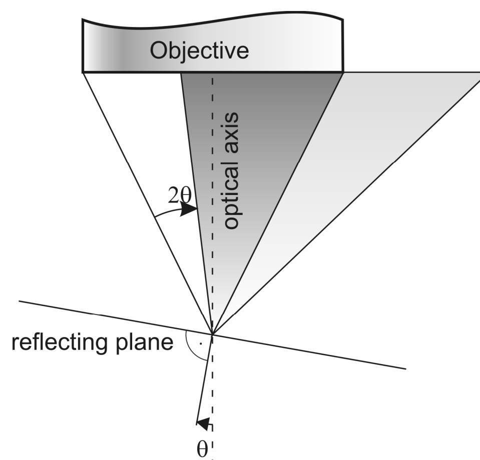

Figure 1. Problem of direct light reflection at the tilted areas

The critical angle depends on the numeric aperture (NA) of the objective. Its theoretical value can be computed as $\alpha_{\max} = \arcsin(NA)/2$. So, for the best non-immersed objectives with NA = 0.95 the critical angle is limited to 36°.
The advantage of the SEM comparing to other measuring techniques is clearly the higher lateral resolution (approx. 5 nm). The surface information exists even for tilt angles of up to 80°. It produces, however, a 2D-Image, so in order to obtain the surface’s height information it is necessary to use several SEM – photos. Currently, there exist 2 classes of methods for converting several 2D images into the real 3D surface.

2. STEREOMETRIC EVALUATION

The 3D - Surface detection can be realized via evaluation of the stereometric image sequence of the specimen. For evaluation all methods require at least 2 images taken at different inclination angles of the specimen. The vertical resolution depends on the lateral resolution and on the tilt angle as follows:

$$R_v = \frac{R_h}{\sin(\lambda)} \tag{1}$$

where R_v is the vertical resolution, R_h is the horizontal resolution, and λ states the tilt angle.
Unfortunately, the inclination angle of the specimen is restricted to approximately 10°, due to the limited contrast ration of the SEM images. (Figure 2). The typical angle of inclination, in which images are still similar, lies within the range of 5 – 7°. By these angles the vertical resolution is approximately 10 times larger than the lateral resolution. To reach a vertical resolution of 0.05 µm, the lateral resolution must lie within the range of 5 nm. Such a high lateral resolution is close to the limit of the SEM - recording technology. Additionally, the final 3D images would have a maximum size of 10 µm x 10 µm, which is insufficient for many structures.

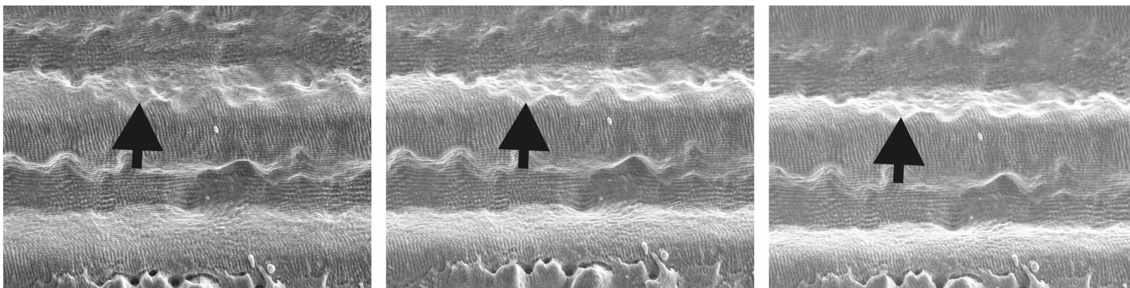

Figure 2. SEM - images with different inclination angle. Arrows mark identical points in the topography whose similarity is no more recognizable particularly in the right image.

3. PHOTOMETRIC METHOD

A photometric method uses dependence of the secondary/backscattered electrons yield on the inclination angle of the irradiated area. Before the algorithm is introduced, let us discuss physical processes occurring during irradiation by primary electrons.

3.1 Physical processes

The energy of the primary electrons (PE) lies in the range of 0.5-30 keV. Electrons penetrated in the surface create an electron diffusion region. Depending on the activation type free electrons of different energy level are being produced. Inelastic scattering of the primary electrons in the area close to the injection hole (1-10 nm) results in creation of the low-energy, the so called pure secondary electrons SE1. The energy of these electrons lies per definition in the range of 0-50eV. Backscattered (BSE) electrons with energies > 50eV also produce low energy secondary electrons, so called SE2. The source area for SE2 as well as for BSE is much larger and depends on the energy of the primary electrons and the irradiated material (Figure 3). So, for the PE-energy of 10-20 keV the diameter of the excited spot of the surface lies in the range of 0.1- 1μm and it decreases to 5-50 nm at lower energies. The BSE can also produce SE3 while contacting the chamber walls. However, these electrons can be eliminated and therefore will be not discussed in this paper anymore.

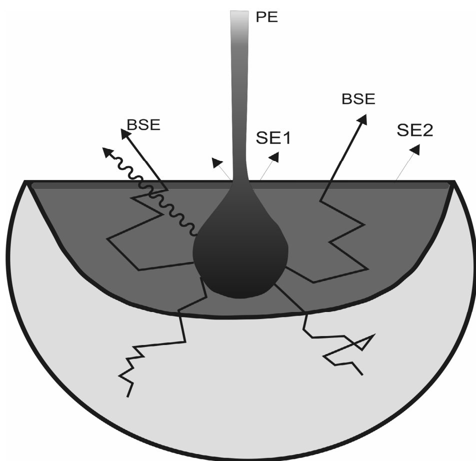

Figure 3. Excitation of secondary and backscattered electrons

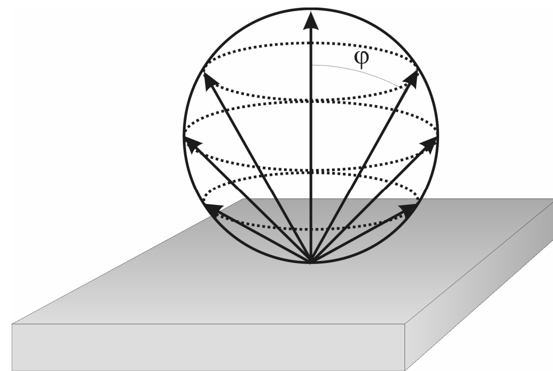

Figure 4. Emission of the electrons according to Lambert's law

As already mentioned, the total amount of electrons σ consists of the SE1 - yield δ and of the SE2-yield, which can be described via the number of the backscattering (BSE) coefficient η. Thus, the total amount of SE electrons can be expressed as:

$$\sigma = \delta + \beta \cdot \eta \tag{2}$$

Here β is the coefficient that depends on the material of the irradiated sample and on the energy of the primary electrons. For PE-energy > 5keV this factor lies in the range of 2-3. The dependence of the BSE - coefficient η on the inclination angle of the specimen can be described via following empirical formula [Reimer 1998]

$$\eta(Z,\varphi) = (1+\cos\varphi)^{-9/\sqrt{Z}} \tag{3}$$

The BSE - coefficient also depends on the material. For high atomic numbers Z, for example Au or Cu, it strongly decreases for low PE-energies (below 5keV). [Reimer 1998]. The SE1-yield δ also depends on the inclination angle of the sample and on the energy of the primary electrons (E) as:

$$\delta(\varphi) = \sec^{\lambda}\varphi, \qquad \delta(E) \sim E^{-0.8} \tag{4}$$

All these observations show that the best results in surface reconstruction can be achieved via analysis of the secondary electrons in low voltage scanning electron microscope (LVSEM). For registering these electrons the Everhart-Thornley detector can be used (Figure 5)

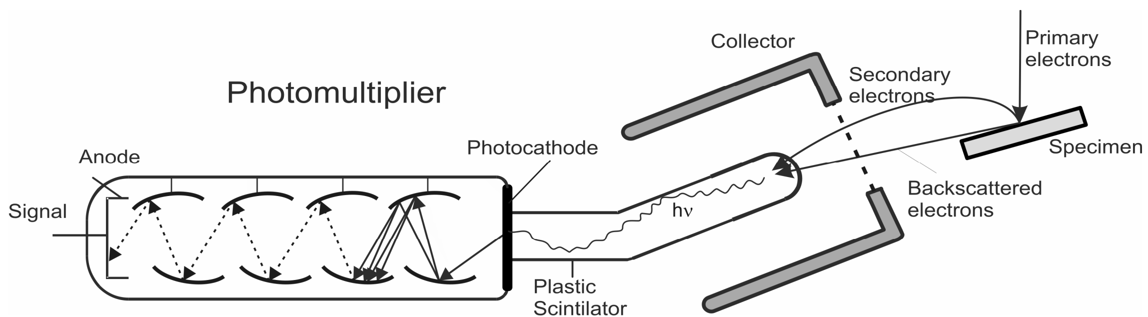

Figure 5. Everhart-Thornley SE-detector

The BSE-electrons can also be used for the surface reconstruction. However, their energies and therefore the velocities are so high that their trajectories take the form of the straight line. Due to the fact, that BSE detectors do not cover all directions, not all BSE are being registered, and the whole amount of the BSE electrons cannot be properly evaluated.

The last two important laws, which are used for the surface reconstruction, are the angle dependence of the emitted electrons and their energy distribution. According to Lambert's cosine law, the angle distribution of the probability density takes the following form:

$$f(\varphi) = \frac{1}{\pi}\cos\varphi \tag{5}$$

where φ - angle between normal vector to the surface and investigated direction (Figure 4)

The typical energy distribution of SE's is shown on Figure 6. According to [Reimer 1993] the probability density of the secondary electrons as function of the electron's energy can be approximated as:

$$f(U_e) = K(U_p)\frac{U_e}{\left(U_e + W_e\right)^4}, K(U_p) = \frac{6W_e^2\left(U_p + W_e\right)^3}{U_p^3 + 3U_p^2 W_e} \tag{6}$$

where W_e - electron's work function, E_p - energy of the primary electrons.

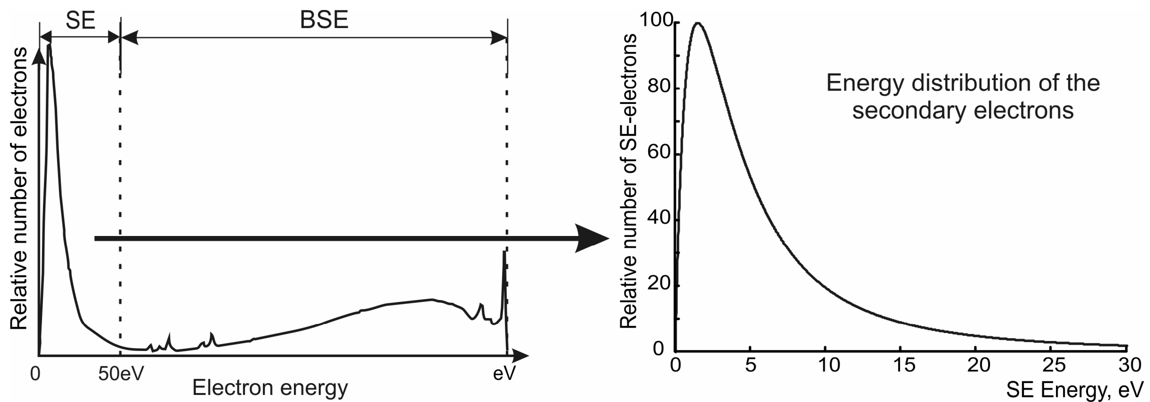

Figure 6. Energy distribution of the secondary electron's yield

3.2 Surface analysis

For the surface reconstruction 4 Everhart-Thornley SE-detectors are used. They are symmetrically positioned in the Z0X and ZOY planes. The tilt angle of each detector is φ_0 (Figure 7).

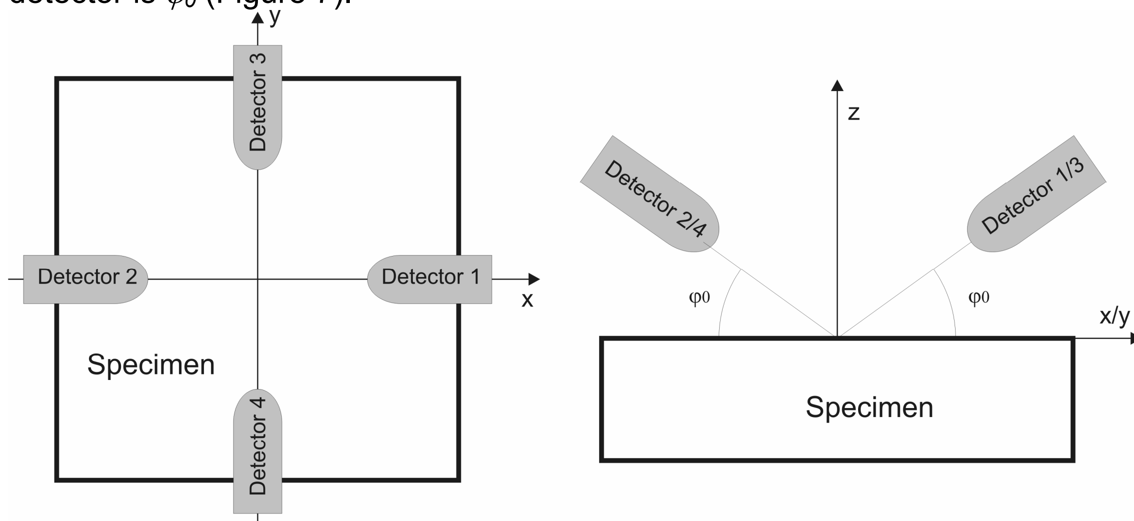

Figure 7. Hardware configuration

The method for the surface reconstruction in 2D space was presented in [Böngeler 1987]. However, due to the fact, that most of the structures have inhomegeneities in x and y directions, it should be extended into the 3rd dimension.

The bias voltage on the collector grid should be sequentially applied on two opposite pairs. Under the assumption that the trajectories of the emitted electrons are not affected by the disturbance of the electric field near the

surface, all electrons with initial velocity vector with a positive x-projection should be registered with detector 1/3. The electrons with a negative projection of the velocity vector should be registered with detector 2/4 (Figure 8).

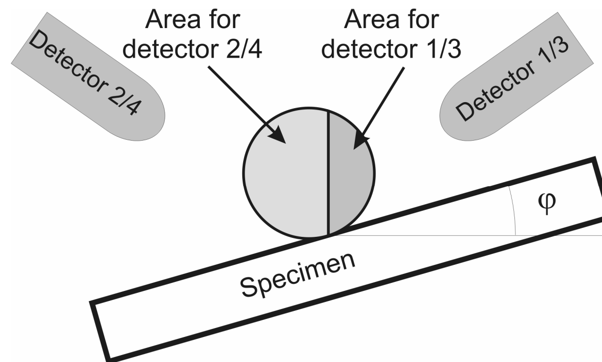

Figure 8. Detection of the electrons

Hence, the signal distribution for the convex surfaces should take the following form:
Detector 1/3:

$$I_{1,3}=\frac{\sigma(\varphi)}{2}(1-\sin\varphi) \tag{7}$$

Detector 2/4:

$$I_{2,4}=\frac{\sigma(\varphi)}{2}(1+\sin\varphi) \tag{8}$$

In reality surface consists not only of convex areas but also of concave ones. In this case some electrons re-penetrate into the specimen and therefore are not detected. The fraction of these electrons can be calculated using the following expression:

$$\psi(x,y)=1-\frac{1}{\pi}\int_0^{2\pi}d\alpha\int_0^{\varphi_{\max}(x,y,\alpha)}\cos(\varphi)\sin(\varphi)\,d\varphi=\frac{1}{2}+\frac{1}{4\pi}\int_0^{2\pi}\cos\left(2\varphi_{\max}(x,y,\alpha)\right)d\alpha= \\ \frac{1}{4\pi}\int_0^{2\pi}\cos^2\left(\varphi_{\max}(x,y,\alpha)\right)d\alpha \tag{9}$$

where $\varphi_{max}(\alpha)$ states the maximal angle between normal vector to the surface and the tangent line (Figure 9)

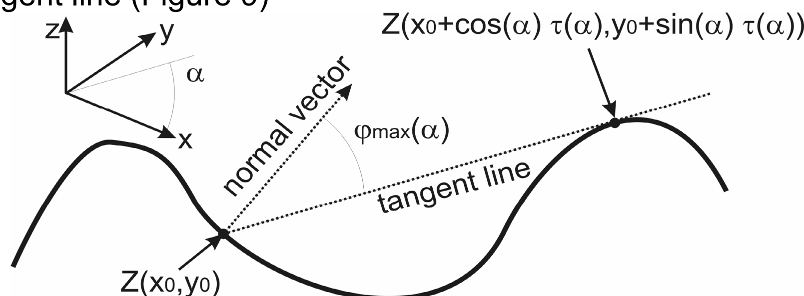

Figure 9. Evaluation of the non-detectable electrons fraction

Assuming that the surface of the specimen can be presented as continuously differentiable function *Z(x,y)*, function $\varphi_{max}(x,y,\alpha)$ from the Eq. 9 can be expressed as:

$$\cos(\varphi_{max}) = \frac{\left(\frac{\partial Z(x,y)}{\partial x}\cos\alpha + \frac{\partial Z(x,y)}{\partial y}\sin\alpha\right)\cdot\tau(\alpha) + Z(x+\tau(\alpha)\cos\alpha, y+\tau(\alpha)\sin\alpha) - Z(x,y)}{\sqrt{1+\frac{\partial Z(x,y)}{\partial x}^2+\frac{\partial Z(x,y)}{\partial y}^2}\sqrt{\tau^2(\alpha)+\left(Z(x+\tau(\alpha)\cos\alpha, y+\tau(\alpha)\sin\alpha)-Z(x,y)\right)^2}} \quad (10)$$

Here $\tau(\alpha) = \tau(x,y,\alpha) = \left\{\tau > 0, \frac{Z(x+\tau\cos\alpha, y+\tau\sin\alpha) - Z(x,y)}{\tau} = \max\right\}$ denotes the distance between point (x,y) and the point $(x+\tau(\alpha)\cos\alpha, y+\tau(\alpha)\sin\alpha)$ that corresponds to the maximal inclination of the straight line, connecting point (x,y) and all points $Z(x+\tau\cos\alpha, y+\tau\sin\alpha)$. This function is determined via step-by-step tabulation of the function $Z(x+\tau\cos\alpha, y+\tau\sin\alpha)$.

Hence, the fraction of undetectable electrons for detectors corresponds to:

$$\kappa_{1...4}(x,y) = \frac{1}{4\pi}\int_a^b \cos^2(\varphi_{max}(x,y,\alpha))\,d\alpha \quad (11)$$

The integration limits depend on the detector and take on the following values for given setup:

Detector 1: $[0,\pi]$, Detector 2: $[\pi/2, 3\pi/2]$

Detector 3: $[\pi, 2\pi]$, Detector 4: $[3\pi/2, 5\pi/2]$

The signals, calculated in (7), (8) should be corrected as follows:

$$\kappa_{1...4}(x,y) = \frac{1}{4\pi}\int_a^b \cos^2(\varphi_{max}(x,y,\alpha))\,d\alpha \quad (12)$$

Combining Eq.12 and the definition of the surface's gradient follows to:

$$\begin{cases} \frac{I_2 - I_1}{I_1 + I_2} = \left(\frac{\frac{\partial Z}{\partial x}}{\sqrt{1+\frac{\partial Z}{\partial x}^2}} - \kappa_2(x,y) + k_1(x,y)\right) \Big/ \left(1 - \kappa_1(x,y) - k_2(x,y)\right) \\ \frac{I_4 - I_3}{I_3 + I_4} = \left(\frac{\frac{\partial Z}{\partial y}}{\sqrt{1+\frac{\partial Z}{\partial y}^2}} - \kappa_4(x,y) + k_3(x,y)\right) \Big/ \left(1 - \kappa_3(x,y) - k_4(x,y)\right) \end{cases} \quad (13)$$

The standard approach, shown for example in [Böngeler 1987], [Slowko 2006] assumes that σ(φ)=sec(φ) and therefore the area can be evaluated as $\tan(\varphi)=Z'_x=I_2-I_1$. However, it is not true for arbitrary materials (see Eq. 2 - Eq.4) and surfaces (the inclination angle incorporates Z'_x and Z'_y simultaneously).

The solution of this equation system leads to evaluation of the partial derivations of the surface function in x and y directions respectively. Numerical integration yields the unknown area surface.

Because of the fact that the surface is initially unknown, the correction parameters cannot be determined properly. That is why the procedure of the

surface reconstruction should use the iterative scheme. Firstly, no correction will be done. The surface, obtained after the first iteration, will be used for evaluation of the re-penetrating electron fraction $\kappa_1 ... \kappa_4$. Newly calculated fractions are used for evaluation of the surface $Z(x,y)$. In the case of simple structures 3-5 iterations are sufficient for reconstruction of the true surface.

4. FINAL REMARKS

In reality, the trajectories of the secondary electrons are influenced by the distortions of the electric field near conductive surfaces. So, the real fraction of the non-detectable electrons varies slightly from calculated in Eq. 11 value. Therefore final iteration should calculate this fraction more precisely. For this purpose the FEM-simulations can be used. For these simulation it is necessary to know not only the angle, but also the initial velocity distributions that are given in Eq. 6.

System with 4-Everhart-Thornley detectors can be substituted with 2-detector system and the rotation unit. The system with one detector is also possible, but in this case the amount of the detected electrons cannot be calculated via given formulas. As shown in [Konvalina 2006] the electric field distribution becomes very complicated due to the influence through body of electrons gun, chamber wall etc.

5. REFERENCES

[Reimer 1993] Reimer, L.; "Image Formation in Low-Voltage Scanning Microscopy"; SPIE Optical Engineering Press 1993; ISBN 0-8194-1206-6

[Böngeler 1987] Reimer, L.; Böngeler, R.; Desai, V.; "Shape From Shading Using Multiple Detector Signals in Scanning Electron Microscopy"; In: *Scanning Microscopy*, Vol. 1, No. 3, 1987, pp. 963-973

[Reimer 1998] Reimer, L.; "Scanning Electron Microscopy. Physics of Image Formation and Microanalysis"; Springer Verlag Berlin Heidelberg, 1998; ISBN 3-540-639756-4

[Slowko 2006] Paluszynski, J.; Slowko, W.; "Compensation of the shadowing error in three-dimensional imaging with a multiple detector scanning electron microscope"; In: *Journal of Microscopy*, pp. 93-96; 2006

[Konvalina 2006] Konvalina, I.; Müllerova, I.; "The Trajectories of Secondary electrons in the Scanning Electron Microscope"; In: Scanning. Vol. 28, pp. 245-256